# Restricted Constrained Delaunay Triangulations

**Marc Khoury**
University of California at Berkeley, CA, USA

**Jonathan Richard Shewchuk**
University of California at Berkeley, CA, USA

## Abstract

We introduce the restricted constrained Delaunay triangulation (restricted CDT), a generalization of both the restricted Delaunay triangulation and the constrained Delaunay triangulation. The restricted CDT is a triangulation of a surface whose edges include a set of user-specified constraining segments. We define the restricted CDT to be the dual of a restricted Voronoi diagram defined on a surface that we have extended by topological surgery. We prove several properties of restricted CDTs, including sampling conditions under which the restricted CDT contains every constraining segment and is homeomorphic to the underlying surface.

**2012 ACM Subject Classification** Theory of computation → Randomness, geometry and discrete structures

**Keywords and phrases** restricted Delaunay triangulation, constrained Delaunay triangulation, surface meshing, surface reconstruction, topological surgery, portals

**Digital Object Identifier** 10.4230/LIPIcs.SoCG.2021.49

**Related Version** *Complete version*: `https://people.eecs.berkeley.edu/~jrs/papers/rcdt.pdf`

**Funding** Supported in part by the National Science Foundation under Awards CCF-1423560 and CCF-1909204 and in part by a National Science Foundation Graduate Research Fellowship.

**Acknowledgements** This work was initiated at the Workshop on Geometric Algorithms in the Field hosted by the Lorentz Center in Leiden, the Netherlands during June 2014. We thank the organizers – Sándor Fekete, Maarten Löffler, Bettina Speckmann, and Jo Wood – and the Lorentz Center for providing accommodations. We especially thank Bruno Lévy for posing the problem this paper answers, Marc van Kreveld for helpful discussions, and the referees for improving the paper.

## 1 Introduction

The constrained Delaunay triangulation (CDT) in the plane [19, 25, 13] is a popular geometric construction that shares some of the advantages and mathematical properties of the Delaunay triangulation, but also permits users to constrain specified edges to be part of the triangulation. CDTs are used in applications such as computer graphics, geographical information systems, and guaranteed-quality mesh generation algorithms [12]. Our goal here is to offer a mathematically rigorous way to define a Delaunay-like triangulation on a curved surface embedded in three-dimensional space, with the same ability to constrain edges.

Another variant of the Delaunay triangulation, called the *restricted Delaunay triangulation* (RDT), has become a well-established way of generating triangulations on curved surfaces [16]. RDTs have equipped theorists to rigorously prove the correctness of algorithms for surface reconstruction [14] and surface mesh generation [12]. In this paper we introduce *restricted constrained Delaunay triangulations* (restricted CDTs), which combine ideas from CDTs and RDTs to enable the enforcement of constraining edges in RDTs.

Think of the restricted CDT as a function that takes in three inputs: a compact, smooth surface $\Sigma \subset \mathbb{R}^3$ without boundary; a finite set $V \subset \Sigma$ of points (called *sites* or *vertices*); and a finite set $S$ of line segments whose endpoints are in $V$. If certain conditions on the density


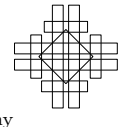

of $V$ and the lengths of the segments are met then, as illustrated in Figure 1, the output is a simplicial complex $\mathcal{T}$ such that the set of vertices of $\mathcal{T}$ is $V$, the set of edges of $\mathcal{T}$ is a superset of $S$, and $\mathcal{T}$ is a triangulation of $\Sigma$. The last phrase means that the *underlying space* of $\mathcal{T}$, written $|\mathcal{T}| = \bigcup_{\tau \in \mathcal{T}} \tau$, is homeomorphic to $\Sigma$.

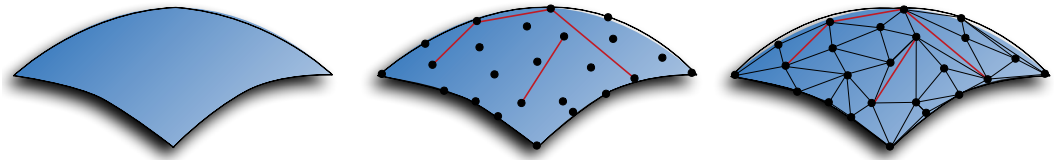

**Figure 1** Given a set of points sampled from a surface $\Sigma$ and a set of segments, red, we wish to compute a triangulation of $\Sigma$ that contains all of the red segments.

Although Delaunay triangulations in the plane can be constrained to include arbitrary edges, the same is not true of three-dimensional Delaunay triangulations; consider the fact that not all nonconvex polyhedra can be tetrahedralized [24]. Nor is it always possible to constrain arbitrary edges to be part of a surface triangulation. Our challenge is to establish conditions on the input that guarantee that a suitable triangulation exists.

We follow the example of the RDT, which is defined by dualizing a *restricted Voronoi diagram*. Given inputs $\Sigma$ and $V$ (but no segments), the *restricted Voronoi cell* of a site $v \in V$, denoted $\mathrm{Vor}|_\Sigma v$, is the set of all points on $\Sigma$ for which $v$ is the closest site in $V$ (possibly tied for closest), as measured by the Euclidean distance in $\mathbb{R}^3$. Equivalently, $\mathrm{Vor}|_\Sigma v = \mathrm{Vor}\, v \cap \Sigma$, where $\mathrm{Vor}\, v$ is $v$'s standard Voronoi cell in $\mathbb{R}^3$. The name "restricted Voronoi cell" arises because $\mathrm{Vor}|_\Sigma v$ is the restriction of $\mathrm{Vor}\, v$ to the surface $\Sigma$.

A *restricted Voronoi face* is any nonempty set of points found by taking the intersection of one or more restricted Voronoi cells. The *restricted Voronoi diagram* $\mathrm{Vor}|_\Sigma V$ is the cell complex containing all the restricted Voronoi cells and faces.

The *restricted Delaunay triangulation* $\mathrm{Del}|_\Sigma V$ is the simplicial complex dual to $\mathrm{Vor}|_\Sigma V$. If the restricted Voronoi cells of two sites $v, w \in V$ have a nonempty intersection (typically a path on $\Sigma$), then $vw$ is a *restricted Delaunay edge* in $\mathrm{Del}|_\Sigma V$. If the restricted Voronoi cells of three sites $u, v, w \in V$ have a nonempty intersection (typically a single point on $\Sigma$, called a *restricted Voronoi vertex*), then $\triangle uvw$ is a *restricted Delaunay triangle* in $\mathrm{Del}|_\Sigma V$. Every site in $V$ is a vertex in $\mathrm{Del}|_\Sigma V$. Note that $\mathrm{Del}|_\Sigma V$ may not be a valid simplicial complex unless $V$ is a sufficiently dense sample of $\Sigma$, perhaps with suitable perturbations of $\Sigma$ and $V$. See Section 3 for a more nuanced discussion.

To modify RDTs so that we can constrain edges, we borrow from Seidel [25] the idea of an *extended Voronoi diagram*, which is the natural dual of the CDT in the plane. Seidel performs a topological surgery on the plane in which each segment in $S$ becomes a slit cut in the plane; upon these slits he glues topological extensions called "secondary sheets" on which additional portions of the extended Voronoi diagram are drawn. Likewise, we perform surgery by cutting slits in the surface $\Sigma$ and grafting independent new surfaces called *extrusions* onto $\Sigma$ at these slits. We think of these slits as *portals*: an ant crawling on the surface across a constraining edge finds itself transported by the portal to a secondary space where the extended surface continues along an infinite extrusion.

A key contribution of this paper is our definition of the restricted constrained Delaunay triangulation, as the dual of the Voronoi diagram restricted to this surgically extended surface. Another contribution is to prove several properties of restricted CDTs, including conditions under which the restricted CDT contains every constraining edge, conditions under which the restricted CDT is homeomorphic to the underlying surface $\Sigma$, and a characterization of which vertices must be considered to compute the triangles near a segment.

Shewchuk [26] demonstrates that for Delaunay mesh generators that create high-quality meshes of domains in the plane with constraining segments, the use of a CDT (rather than a pure Delaunay triangulation) reduces the number of triangles and vertices – on some domains, by as much as 25%. He also proves that there is a theoretical advantage: Delaunay meshing with a CDT offers a guarantee of a "size optimal" mesh with no angle less than 26.56°, whereas an *unconstrained* Delaunay triangulation offers a weaker guarantee, a size optimal mesh with no angle less than 20.7°. It is very likely that surface meshing algorithms based on restricted CDTs can offer the same advantages, compared to what pure RDTs can achieve.

An alternative approach sometimes suggested is to define a Voronoi diagram based on an intrinsic (geodesic) distance metric, then obtain a triangulation by duality. This idea is mathematically elegant, but computing a geodesic Voronoi diagram entails numerical approximation algorithms [18, 20, 21], which add coding complexity and running time. RDTs are popular in surface mesh generation because they are easier to compute. We emphasize that although our construction of restricted CDTs may seem complicated, it is in the service of producing simple algorithms. (In particular, Theorems 1 and 3 simplify computing the triangles near a segment.) See Section 6 for some speculation on prospective algorithms.

## 2 Portals and topological surgery

Informally, a *portal* $P$ is a doorway between two topological spaces, with $P$ shared by both. Our main topological construction starts with disjoint topological spaces $Y$ and $Z$, then glues them together into a single space by specifying an equivalence relationship between a subset of points $P \subset Y$ and a subset $P' \subset Z$. For clarity, we explain Seidel's construction of portals in the plane [25] first, then our construction of portals and an extended surface in $\mathbb{R}^3$.

### 2.1 Portals and extended Voronoi diagrams in the plane

Let $X = \mathbb{R}^2$ and let $S$ be a finite set of line segments in the plane; the segments may intersect each other only at their endpoints. Consider a segment $s = pq \in S$ (meaning $s$ has endpoints $p$ and $q$). The relative interior of $s$, denoted $\operatorname{relint} s$, consists of all points on $s$ except $p$ and $q$. Let the *slitted plane* $X_s = X - \operatorname{relint} s$ be the plane with the relative interior of $s$ removed. The affine hull of $s$ has two "sides." Our goal is to augment $X_s$ by gluing it to two additional topological spaces, one for each side of $s$, along the slit created by removing $\operatorname{relint} s$. The three spaces are glued together along two portals, each of which is topologically a copy of $s$. Thus an ant crawling on the extended space that crosses $s$ from one side finds itself in a *secondary branch*; and an ant that crosses $s$ from the other side finds itself in a different secondary branch. After repeating this augmentation for every segment in $S$, we can draw on the extended space an *extended Voronoi diagram* whose dual is the CDT.

Topologically, $X_s$ has a hole such that $X_s$ is *almost* an open set, except that $X_s$ has two boundary points, $p$ and $q$. We want to glue two additional spaces to $X_s$ – one for each side of $s$ – so we augment $X_s$ with additional points that serve as two portals to those additional spaces. We define a closed topological space $\overline{X}_s$ by augmenting $X_s$ with two connected curves $\zeta^+$ and $\zeta^-$, called *portals*, that together serve as the boundary of the hole. Each of $\zeta^+$ and $\zeta^-$ has $p$ and $q$ as its endpoints, but the two curves share no other points. In essence, the portals are copies of $s$ with shared endpoints. Formally, $\overline{X}_s$ is the completion of the incomplete metric space $X_s$ with respect to the shortest-path metric in $X_s$.

The points in $X_s$ inherit Cartesian coordinates from the plane, and the points on the portals $\zeta^+$ and $\zeta^-$ inherit Cartesian coordinates from the segment $s$. Two points in $\overline{X}_s$ – one on $\zeta^+$ and one on $\zeta^-$ – can have the same $(x, y)$-coordinate values yet be topologically distinct.

Let $\mathbb{R}^2_-$ and $\mathbb{R}^2_+$ be two copies of $\mathbb{R}^2$. We treat $\overline{X}_s$, $\mathbb{R}^2_-$, and $\mathbb{R}^2_+$ as three distinct topological spaces that all inherit the Cartesian coordinate system – so two points in two different spaces can have the same coordinate values yet be topologically distinct.

Informally, we glue $\mathbb{R}^2_+$ to $\overline{X}_s$ along $\zeta^+$ and glue $\mathbb{R}^2_-$ to $\overline{X}_s$ along $\zeta^-$. Formally, we write $x \equiv y$ if $x$ and $y$ have the same coordinate values, even though they may lie in different spaces. Let $p$ and $q$ be the endpoints of $s$. Define an equivalence relation $\sim$ as

$$x \sim y \iff \begin{cases} x = y & x, y \in \overline{X}_s \text{ or } x, y \in \mathbb{R}^2_+ \text{ or } x, y \in \mathbb{R}^2_-, \\ x \equiv y & x \in \mathbb{R}^2_+ \text{ and } y \in \zeta^+, \\ x \equiv y & x \in \mathbb{R}^2_- \text{ and } y \in \zeta^-, \\ x \equiv p \equiv y \text{ or } x \equiv q \equiv y & x \in \mathbb{R}^2_+ \text{ and } y \in \mathbb{R}^2_-. \end{cases} \tag{1}$$

With $\sim$ we construct the quotient space $\widetilde{X} = (\overline{X}_s \sqcup \mathbb{R}^2_+ \sqcup \mathbb{R}^2_-)/\sim$. We refer to $\overline{X}_s$ as the *principal branch* and refer to $\mathbb{R}^2_+$ and $\mathbb{R}^2_-$ as *secondary branches*. Figures 2 and 3 illustrate this construction. Note that in the quotient space, the endpoints $p$ and $q$ of the segment $s$ are present in, and shared by, all three of the original spaces.

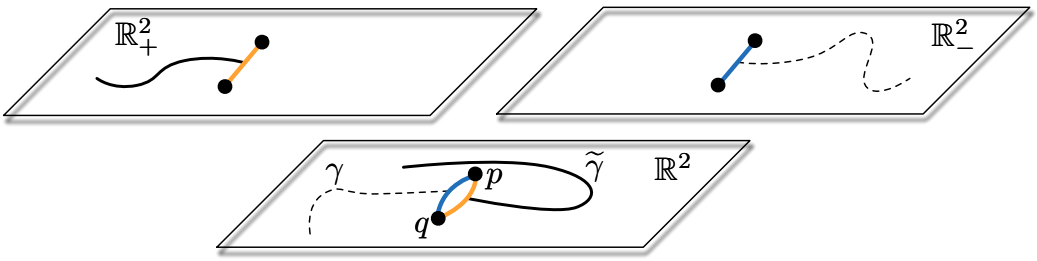


**Figure 2** The completion of the slitted plane has a topological hole bounded by two portals, marked in blue and orange. (Geometrically, the two portals are straight line segments that occupy exactly the same coordinates.) The equivalence relation $\sim$ identifies the blue path in the principal branch with the blue path in $\mathbb{R}^2_-$; likewise the two orange paths become one. A path in the principal branch (bottom) that enters a portal continues in the appropriate secondary branch.

The construction works for any finite number $m = |S|$ of non-crossing segments. Let $X_S = X - \bigcup_{s \in S} \operatorname{relint} s$. Let $\overline{X}_S$ be the completion of $X_S$ with respect to the shortest-path metric in $X_S$, which adds two portals for each segment. Then we construct a quotient space $\widetilde{X}$ composed of $\overline{X}_S$ and $2m$ copies of $\mathbb{R}^2$ glued along the $2m$ portals bounding the $m$ holes in $\overline{X}_S$.

For the sake of defining the Voronoi diagram of a finite set of sites in $\widetilde{X}$, Seidel [25] defines a distance function on $\widetilde{X}$ which is essentially the Euclidean distance, except that the distance between two points is infinite if they are not visible from each other. (Note that this distance function is not a metric.) A path $\gamma \subset \widetilde{X}$ may pass through portals and visit secondary branches, but because of the slits we have cut in $X_S$, $\gamma$ cannot cross the relative interior of a segment without being transported by a portal. We call a path *straight* if its Cartesian embedding is a straight line segment. Two points $p, q \in \widetilde{X}$ are *visible* from each other if there is a straight path $\gamma \subset \widetilde{X}$ with endpoints $p$ and $q$. The distance $\widehat{d}(p, q)$ from $p$ to $q$ is the Euclidean distance if $p$ and $q$ are visible from each other; otherwise, $\widehat{d}(p, q) = \infty$.

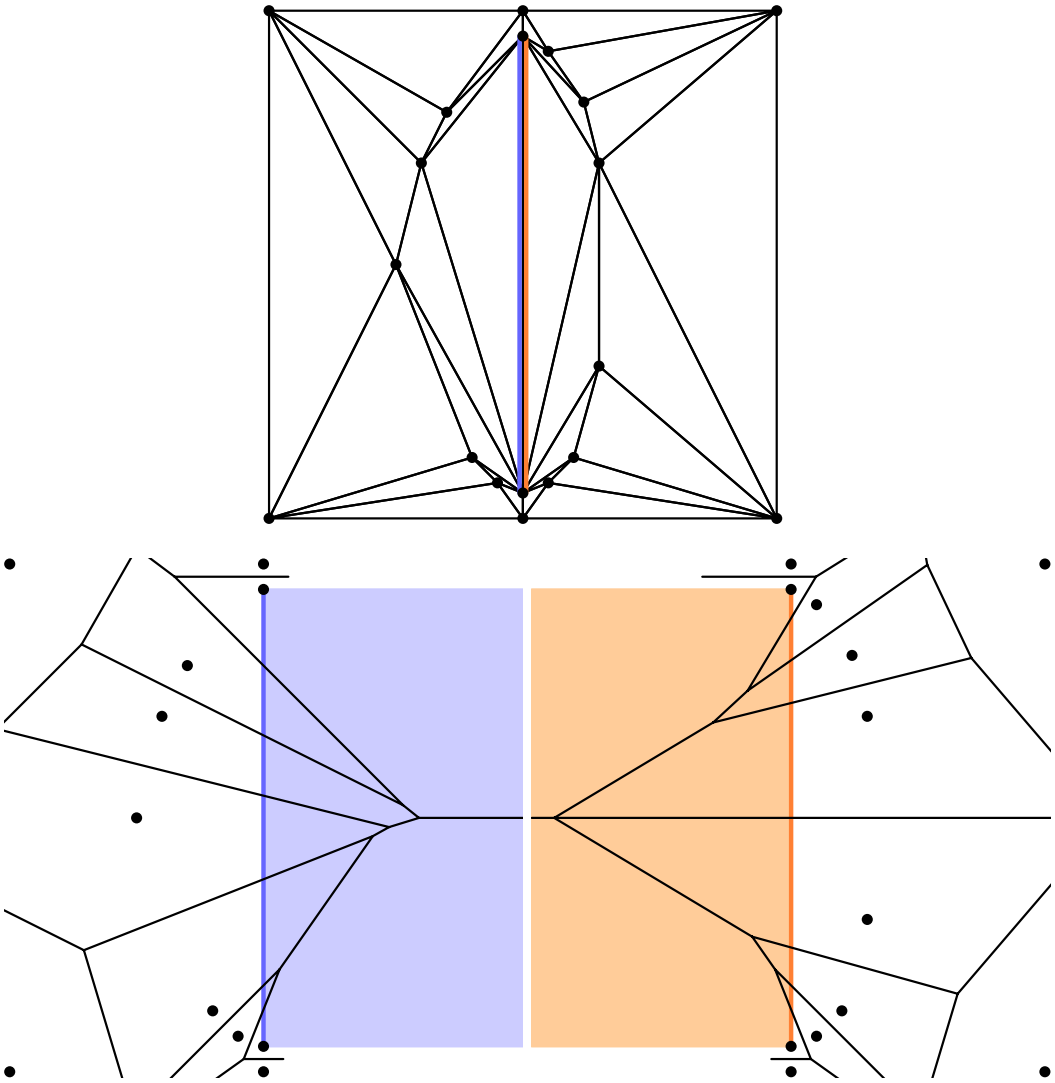

**Figure 3** A one-segment CDT (top) and its dual extended Voronoi diagram (bottom). The blue and orange regions show the portions of the Voronoi diagram on the secondary branches.

The extended Voronoi diagram assigns each point in $\widetilde{X}$ to (the Voronoi cells of) one or more sites in $V$. Those sites must be visible from the point; no site can claim a point it cannot see. If a point on a secondary branch is claimed by a site other than the branch's portal's endpoints, the site is visible from the point through the portal, as Figure 3 illustrates. Seidel gives an algorithm for constructing the extended Voronoi diagram, and by duality the CDT.

## 2.2 Portals on surfaces embedded in $\mathbb{R}^3$

A similar construction works for a compact, smooth surface without boundary $\Sigma \subset \mathbb{R}^3$. However, whereas in the plane we construct one new topological space, here we will require two. We surgically augment the surface $\Sigma$ by cutting slits along *portal curves*, one for each segment, and gluing two *extrusions* onto each portal curve, yielding an *extended surface* $\widetilde{\Sigma}$. The purpose of this extended surface is to serve as a canvas upon which we can draw an extended restricted Voronoi diagram, which we dualize to define a restricted CDT.

To define a Voronoi diagram we need a distance function, and $\widetilde{\Sigma}$ alone does not provide one that is easily computed. While an intrinsic (geodesic) distance might be ideal in principle, for the sake of speed and a simple implementation, we use the Euclidean distance in $\mathbb{R}^3$ as RDTs do; but we must modify the Euclidean distance so that the restricted Voronoi diagram respects the input segments. Hence most of our work will be to construct a surgically modified three-dimensional space $\widetilde{X}$ in which we embed $\widetilde{\Sigma} \subset \widetilde{X}$. Like Seidel's extended space in Section 2.1, $\widetilde{X}$ obstructs (and supports) visibility in a manner that is suitable for defining a restricted Voronoi diagram on $\widetilde{\Sigma}$ and makes it easy to compute restricted CDTs.

To define $\widetilde{X}$, we specify portals in $\mathbb{R}^3$ where points will be removed, analogous to cutting slits in the plane. Each portal is a two-dimensional ruled surface with boundary (not generally flat), approximately perpendicular to $\Sigma$. The intersection of a portal with $\Sigma$ is a portal curve. Each portal has two "sides," and on each side we glue an additional copy of $\mathbb{R}^3$ to form $\widetilde{X}$. In each copy of $\mathbb{R}^3$ we embed an extrusion to form $\widetilde{\Sigma}$. The extended Voronoi diagram assigns each point $x$ on $\widetilde{\Sigma}$ to one or more sites in $V$ that are visible from $x$ along straight paths in $\widetilde{X}$.

To define portal geometry, we need several definitions. The *medial axis* $M$ of $\Sigma$ is the closure of the set of all points in $\mathbb{R}^3$ for which the closest point on $\Sigma$ is not unique. Intuitively, the medial axis of $\Sigma$ is meant to capture the "middle" of the region bounded by $\Sigma$. A *medial ball* is a ball whose center lies on $M$ and whose boundary intersects $\Sigma$ (tangentially), but the interior of the ball does not. For any point $x \in \Sigma$, there are one or two medial balls that have $x$ on their boundaries, called *medial balls at* $x$. If there are two, there is one on each side of $\Sigma$. If there is only one, it is enclosed by $\Sigma$.

For $x \in \Sigma$, the *normal line* $\mathcal{L}_x$ at $x$ is the line orthogonal to $\Sigma$ at $x$ with $x \in \mathcal{L}_x$. The *normal segment* $\ell_x$ at $x$ is a line segment or ray whose endpoints lie on $M$, satisfying $x \in \ell_x \subset \mathcal{L}_x$. If there are two medial balls at $x$, the endpoints of $\ell_x$ are the centers of those two medial balls. If there is only one medial ball at $x$, then $\ell_x$ is a ray originating at the medial ball's center.

The *local feature size* function is $\mathrm{lfs} : \Sigma \to \mathbb{R}$, $x \mapsto d(x, M)$ where $d(x, M)$ denotes the Euclidean distance from $x$ to $M$. We require that $\Sigma$ is smooth in the sense that $\inf_{x \in \Sigma} \mathrm{lfs}(x) > 0$. A finite point set $V \subset \Sigma$ is an *$\epsilon$-sample of* $\Sigma$ if for every point $x \in \Sigma$, $d(x, V) \leq \epsilon\, \mathrm{lfs}(x)$. That is, the ball with center $x$ and radius $\epsilon\, \mathrm{lfs}(x)$ contains at least one point in $V$. See Figure 4.

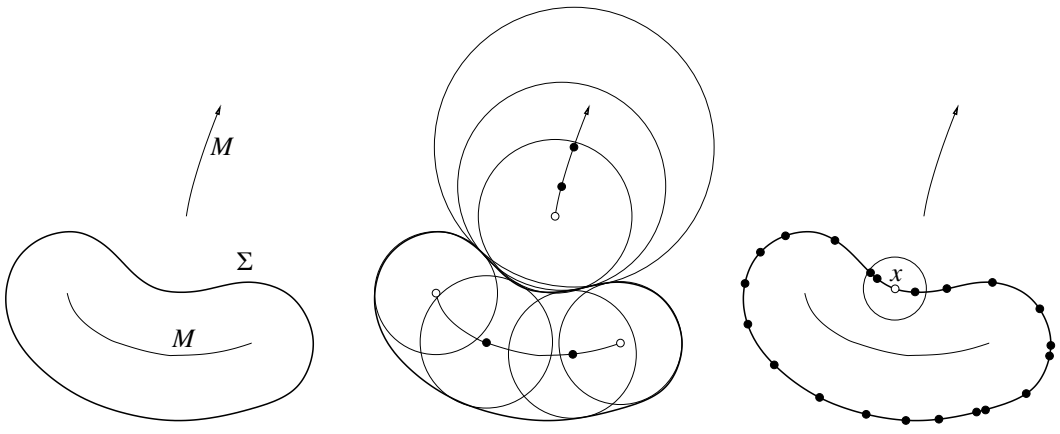


**Figure 4** Left: A 1-manifold $\Sigma$ and its medial axis $M$ (as medial axes in three dimensions are hard to draw or understand). This medial axis is unbounded; one of its components extends infinitely far away. Center: Some of the medial balls that define $M$. Right: A 0.5-sample of $\Sigma$ (filled circles). The ball with center $x$ and radius $0.5\,\mathrm{lfs}(x)$ contains a site.

Let $S$ be a finite set of line segments whose endpoints are in $V$, called the *segments*, which constrain the restricted CDT. Consider a segment $s = pq \in S$ (its endpoints are $p, q \in V$). Let $B_s$ be the *diametric ball* of $s$ – the smallest closed ball such that $s \subset B_s$, so that $s$ is a diameter of $B_s$. Suppose that $d(p,q) \leq \rho\,\mathrm{lfs}(p)$ for some $\rho \in (0,1)$; that is, $s$ is short relative to the local feature size. Then $B_s \cap \Sigma$ is a topological disk [12, Lemma 12.6].

Suppose that we know (or can approximate) the unit vector $n_p$ normal to $\Sigma$ at any site $p$. We choose a *cutting plane* $h_s \supset s$ that is locally orthogonal to the surface $\Sigma$ at $p$ or $q$ (or perhaps somewhere between $p$ and $q$). We use $h_s$ to specify a *portal curve* $\zeta_s = h_s \cap B_s \cap \Sigma$, which is a single connected curve from $p$ to $q$ on $\Sigma$. There is not a canonical choice of cutting plane (and thus portal curve) for $s$, and the user might be presented with a range of choices, but for our presentation here, we choose $h_s = \mathrm{span}\{n_p, \vec{pq}\}$. We require that the portal curves do not cross each other. More precisely, the relative interior of a portal curve may not intersect another portal curve nor a site in $V$.

Our requirement that each portal curve must lie on a plane has both a theoretical motivation and a practical one. The fact that every constraining segment is an edge in the restricted CDT (Theorem 2) depends on the fact that each portal curve lies in a plane and its extrusions are orthogonal to that plane. The requirement simplifies algorithms for computing a restricted CDT, because the Voronoi cells on an extrusion are solely influenced by sites on the other side of the cutting plane – plus the segment endpoints $p$ and $q$. (See Theorem 1.)

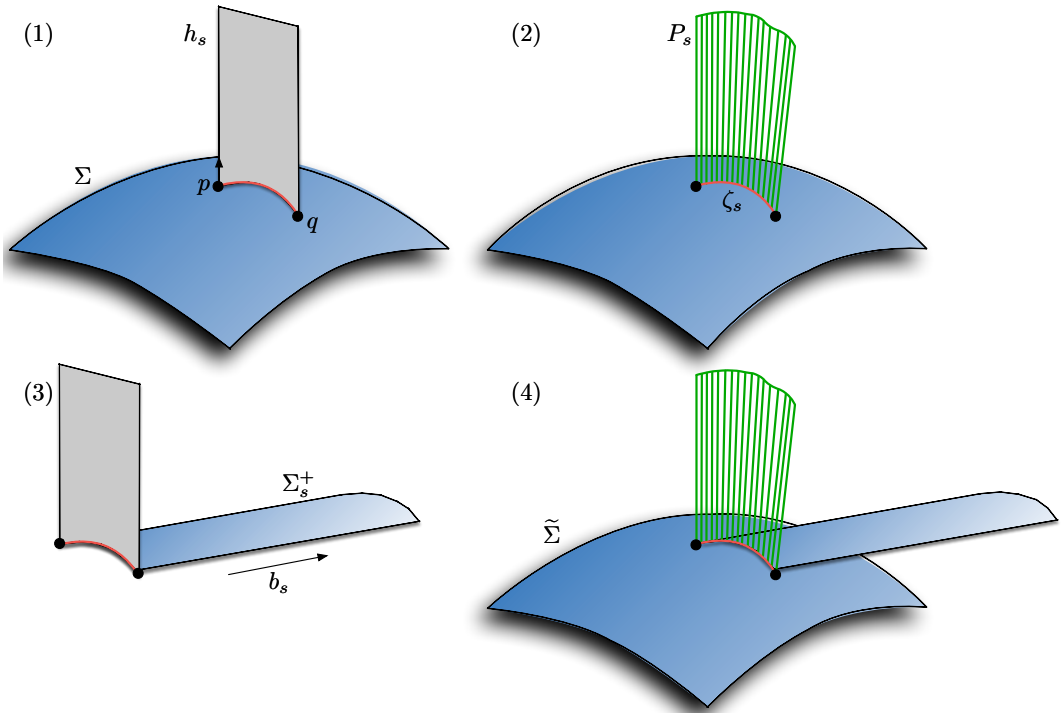


**Figure 5** (1) The plane $h_s$ intersects $\Sigma$ in a curve; the portal curve $\zeta_s$ (red) is the portion of this curve in the diametric ball $B_s$ of the segment $s = pq$. (2) Our portal $P_s$, shown in green, is the union of the normal segments (locally orthogonal to $\Sigma$) of the points on the portal curve $\zeta_s$. The normal segments terminate on the medial axis $M$. (3) We extrude the portal curve $\zeta_s$ into $\mathbb{R}^3_+$ in a direction $b_s$ orthogonal to $h_s$, thus defining $\Sigma_s^+$. (4) We glue the extrusion $\Sigma_s^+$ to $\overline{\Sigma}_S$ (the surface $\Sigma$ with slits cut into it) along $\zeta_s^+$ at the entrance to the portal $P_s^+$.

Figure 5 illustrates our portal construction. For each segment $s$, the portal $P_s = \bigcup_{x \in \zeta_s} \ell_x$ is the union of the normal segments of the points on the portal curve $\zeta_s$. Hence a portal is a ruled surface, topologically two-dimensional but not lying in a plane. Each portal reaches to the medial axis, thereby obstructing visibility so that sites on one "side" of a segment do not influence the restricted Delaunay triangles on the other "side."

If two segments share an endpoint $p$, then their portals share the boundary segment $\ell_p$. The other location where portals' boundaries may intersect each other is at the medial axis. However, no portal intersects the relative interior of another portal.

We construct the extended space $\widetilde{X}$ as we did in Section 2.1, with $P_s$ replacing $s$ and $\mathbb{R}^3$ replacing $\mathbb{R}^2$. Let $X = \mathbb{R}^3$. Let $X_S = X \setminus \bigcup_{s \in S} \operatorname{relint} P_s$, which is $\mathbb{R}^3$ with the relative interior of each portal removed. Let $\overline{X}_S$ be the completion of the incomplete metric space $X_S$ endowed with the shortest path metric. The effect of completing $X_S$ is to augment each "slit" $P_s$ with two portals $P_s^+$ and $P_s^-$, one for each side of $P_s$. These two portals are distinct copies of $P_s$, but $P_s^+$ and $P_s^-$ share a common boundary $\partial P_s = P_s^+ \cap P_s^- = P_s^+ \cap X_S = P_s^- \cap X_S$.

For each segment $s \in S$, let $\mathbb{R}^3_{s+}$ and $\mathbb{R}^3_{s-}$ be two topologically distinct copies of $\mathbb{R}^3$, called *secondary branches*. The points in each secondary branch and the points in the *principal branch* $\overline{X}_S$ all inherit Cartesian coordinates, but points with the same coordinates in different branches are topologically distinct. Define an equivalence relation $\sim$ analogous to (1) that identifies (glues) the points of the portal $P_s^+ \subset \overline{X}_S$ with the points in $\mathbb{R}^3_{s+}$ having the same coordinates, and identifies the points of $P_s^- \subset \overline{X}_S$ with the corresponding points in $\mathbb{R}^3_{s-}$. Thus we glue $2m$ copies of $\mathbb{R}^3$ along the $2m$ portals bounding the $m$ holes in $\overline{X}_S$. The *extended space* is the quotient space $\widetilde{X} = (\overline{X}_S \sqcup \bigsqcup_{s \in S} \mathbb{R}^3_{s+} \sqcup \bigsqcup_{s \in S} \mathbb{R}^3_{s-})/\!\sim$.

Similarly, we surgically modify $\Sigma$ to construct an extended surface $\widetilde{\Sigma} \subset \widetilde{X}$, as shown in the bottom two illustrations in Figure 5. Let $\Sigma_S = \Sigma \setminus \bigcup_{s \in S} \operatorname{relint} \zeta_s$ be the surface with the portal curve interiors removed, and let the *principal surface* $\overline{\Sigma}_S \subset \overline{X}_S$ be its completion. For each $s \in S$, $\overline{\Sigma}_S$ includes two portal curves $\zeta_s^+ \subset P_s^+$ and $\zeta_s^- \subset P_s^-$, one for each side of the cutting plane $h_s$. We extrude $\zeta_s^+$ into $\mathbb{R}^3_{s+}$ and $\zeta_s^-$ into $\mathbb{R}^3_{s-}$, each in one of the two directions normal to the cutting plane $h_s$. Let $b_s$ be a unit vector normal to $h_s$, directed to pass through $P_s^+$ from the principal branch to $\mathbb{R}^3_{s+}$. For each point $x \in \zeta_s$ we define a ray $x_s^+ = \{x + \omega b_s \in \mathbb{R}^3_{s+} : \omega \in [0, \infty)\}$ and a ray $x_s^- = \{x - \omega b_s \in \mathbb{R}^3_{s-} : \omega \in [0, \infty)\}$ (specifying points by their coordinates). We then define two *extrusions*, the ruled surfaces $\Sigma_s^+ = \{x_s^+ : x \in \zeta_s\} \subset \mathbb{R}^3_{s+}$ and $\Sigma_s^- = \{x_s^- : x \in \zeta_s\} \subset \mathbb{R}^3_{s-}$. The *extended surface* is $\widetilde{\Sigma} = (\overline{\Sigma}_S \sqcup \bigsqcup_{s \in S} \Sigma_s^+ \sqcup \bigsqcup_{s \in S} \Sigma_s^-)/\!\sim$.

## 3 Restricted constrained Delaunay triangulations

To define the restricted constrained Delaunay triangulation, we first define the *extended restricted Voronoi diagram* (or just *extended Voronoi diagram* for short) on the extended surface $\widetilde{\Sigma}$. As in Section 2.1, we define a distance function $\widehat{d}(p, q)$ that is the Euclidean distance in $\mathbb{R}^3$ if $p$ and $q$ are visible to each other along a straight path in $\widetilde{X}$, or $\infty$ if they cannot see each other. For any $v \in V$, the *extended restricted Voronoi cell* of $v$ is

$$\operatorname{Vor}|_{\widetilde{\Sigma}} v = \{x \in \widetilde{\Sigma} : \widehat{d}(x, v) \leq \widehat{d}(x, u),\ \forall u \in V\}.$$

An *extended restricted Voronoi face* is any nonempty intersection of one or more extended restricted Voronoi cells. The *extended restricted Voronoi diagram* $\operatorname{Vor}|_{\widetilde{\Sigma}} V$ is the cell complex containing all the extended restricted Voronoi cells and faces.

We define the *restricted constrained Delaunay subdivision* $\operatorname{Del}|_{\widetilde{\Sigma}} V$ to be the polyhedral complex dual to the extended Voronoi diagram in this sense: for each extended Voronoi face $f \in \operatorname{Vor}|_{\widetilde{\Sigma}} V$, let $W \subseteq V$ be the set of sites whose restricted Voronoi cells include $f$ and let $f^*$ be the convex hull of $W$. We say that $f^*$ is the face *dual* to $f$. Then $\operatorname{Del}|_{\widetilde{\Sigma}} V = \{f^* : f \in \operatorname{Vor}|_{\widetilde{\Sigma}} V\}$.

A one-point face in $\mathrm{Vor}|_{\widetilde{\Sigma}} V$ is called an *extended restricted Voronoi vertex*, and its dual is a polygonal or polyhedral face in $\mathrm{Del}|_{\widetilde{\Sigma}} V$, usually a triangle. If an intersection of two extended restricted Voronoi cells includes a path on $\Sigma$, we call it an *extended restricted Voronoi edge*, and its dual is a (straight) *restricted constrained Delaunay edge* in $\mathrm{Del}|_{\widetilde{\Sigma}} V$. Figure 6 illustrates an extended Voronoi vertex on an extrusion and its dual restricted Delaunay triangle, as well as three extended Voronoi edges and their dual restricted constrained Delaunay edges.

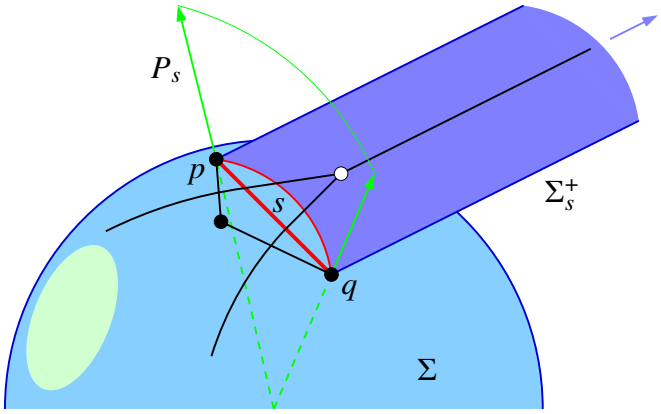


**Figure 6** An extended Voronoi vertex on an extrusion and its dual restricted Delaunay triangle.

If $\mathrm{Del}|_{\widetilde{\Sigma}} V$ contains a polyhedron, we can perturb $\widetilde{\Sigma}$ infinitesimally so that $\widetilde{\Sigma}$ does not pass through the polyhedron's circumcenter; thus with suitable perturbations, $\mathrm{Del}|_{\widetilde{\Sigma}} V$ contains no polyhedra. Relatedly, just as a standard Delaunay triangulation in the plane can be ambiguous if four vertices lie on a common circle, if $V$ has four or more cocircular vertices then $\mathrm{Del}|_{\widetilde{\Sigma}} V$ might contain polygons with four or more sides. If desired, a triangulation can be obtained by subdividing each polygonal face into triangles or by an infinitesimal perturbation of $V$. We recommend the former in practice, but for the sake of our proofs, we will exploit the latter. For simplicity, we will assume in this paper that no point on $\widetilde{\Sigma}$ is equidistant from four visible vertices in $V$; then every polygonal face is a triangle and we can call $\mathrm{Del}|_{\widetilde{\Sigma}} V$ a *restricted constrained Delaunay triangulation* (restricted CDT).

Whereas a restricted Delaunay triangulation (RDT) is a subcomplex of a three-dimensional Delaunay triangulation, we know no natural three-dimensional complex that has the restricted CDT as a subcomplex. One could define a Voronoi diagram over $\widetilde{X}$ and dualize it, but there is no reason to suppose the dual will be a valid polyhedral complex: the Voronoi cells that are supposed to be kept apart by portals are likely to meet near the medial axis. (The dual complex would also be difficult to compute.) The rest of this paper seeks sampling conditions that tame the extended Voronoi diagram (over $\widetilde{\Sigma}$, not $\widetilde{X}$) and its dual restricted CDT.

Now we present several useful properties of extended Voronoi diagrams and restricted CDTs, supposing that no segment is too long. The following theorem shows that the sites whose extended Voronoi cells lie in part on an extrusion $\Sigma_s^+$ must lie on the side of the cutting plane $h_s$ strictly opposite $\Sigma_s^+$ (excepting the endpoints of $s$, which lie on $h_s$). Thus the restricted Voronoi vertices on $\Sigma_s^+$ dualize to restricted Delaunay triangles that are also on the side of $h_s$ opposite $\Sigma_s^+$. This theorem simplifies computing the restricted CDT, because an algorithm only needs to look at sites in one halfspace when computing the portion of $\mathrm{Vor}|_{\widetilde{\Sigma}} V$ that lies on $\Sigma_s^+$. Unfortunately, the proof is five pages long; see the full-length article [17].

▶ **Theorem 1** (Cutting Plane Theorem). *Let $s \in S$ be a segment with endpoints $p, q \in V$ such that $d(p,q) \le \rho\,\mathrm{lfs}(p)$ for $\rho \le 0.47$. Consider a point $x \in \Sigma_s^+$ and a site $v \in V \setminus \{p,q\}$ such that $x \in \mathrm{Vor}|_{\widetilde{\Sigma}} v$. Then $v$ is strictly on the side of $h_s$ opposite $\Sigma_s^+$. (The symmetric claim holds for any $x \in \Sigma_s^-$.)*

The next theorem shows that the restricted CDT $\mathrm{Del}|_{\widetilde{\Sigma}} V$ contains every edge in $S$.

▶ **Theorem 2** (Constraint Theorem). *Let $s \in S$ be a segment with endpoints $p, q \in V$ such that $d(p,q) \le \rho\,\mathrm{lfs}(p)$ for $\rho \le 0.47$. Then $\mathrm{Vor}|_{\widetilde{\Sigma}} p \cap \mathrm{Vor}|_{\widetilde{\Sigma}} q \neq \emptyset$. Hence $pq$ is an edge in $\mathrm{Del}|_{\widetilde{\Sigma}} V$.*

*Moreover, the rays $p_s^+$ and $p_s^-$ lie in the interior of $\mathrm{Vor}|_{\widetilde{\Sigma}} p$ ("interior" with respect to the space $\widetilde{\Sigma}$), and neither ray intersects any other extended restricted Voronoi cell. Likewise, $q_s^+$ and $q_s^-$ lie in the interior of $\mathrm{Vor}|_{\widetilde{\Sigma}} q$, and neither ray intersects another cell.*

**Proof.** We will show that $\mathrm{Vor}|_{\widetilde{\Sigma}} p$ meets $\mathrm{Vor}|_{\widetilde{\Sigma}} q$ on the extrusion $\Sigma_s^+$, as Figures 3 and 6 show. (The same is true on $\Sigma_s^-$.) Let $\Pi$ be the plane orthogonally bisecting $s$. Consider the point $z = \Pi \cap \zeta_s$ on the portal curve and the ray $z_s^+ = \Pi \cap \Sigma_s^+$, whose origin is $z$. Let $x$ be a point on $z_s^+$. Note that $z$ is the point closest to $x$ on the portal plane $h_s$, and $xz$ is perpendicular to $zp$. We will show that for all $x \in z_s^+$ sufficiently far from $z$, $x \in \mathrm{Vor}|_{\widetilde{\Sigma}} p \cap \mathrm{Vor}|_{\widetilde{\Sigma}} q$.

Theorem 1 states that for every site $v \in V \setminus \{p, q\}$ whose extended Voronoi cell $\mathrm{Vor}|_{\widetilde{\Sigma}} v$ intersects $\Sigma_s^+$, $v$ is strictly on the side of $h_s$ opposite $\Sigma_s^+$. Therefore, there exists some $\delta > 0$ such that $d(x,v) \ge d(x,z) + \delta$ for *every* such site $v$. Consider any point $x \in z_s^+$ such that $d(x,z) \ge d(z,p)^2/(2\delta)$. By Pythagoras' Theorem, for every site $v$ whose cell intersects $\Sigma_s^+$,

$$d(x,p)^2 = d(x,z)^2 + d(z,p)^2 \le d(x,z)^2 + 2\delta\, d(x,z) < (d(x,z) + \delta)^2 \le d(x,v)^2.$$

Hence $d(x,q) = d(x,p) < \widehat{d}(x,v)$ for every site $v \in V \setminus \{p,q\}$. As $x$ is visible from $p$ and $q$, $x \in \mathrm{Vor}|_{\widetilde{\Sigma}} p$ and $x \in \mathrm{Vor}|_{\widetilde{\Sigma}} q$. Hence $\mathrm{Vor}|_{\widetilde{\Sigma}} p \cap \mathrm{Vor}|_{\widetilde{\Sigma}} q \neq \emptyset$.

To prove the final claim, consider a point $x \in p_s^+$. Observe that $p$ is the point nearest $x$ on $h_s$ and $d(x,p) < d(x,q)$. Repeating the reasoning above, there exists some $\delta > 0$ such that $d(x,v) \ge d(x,p) + \delta$ for every site $v \in V \setminus \{p\}$ such that $\mathrm{Vor}|_{\widetilde{\Sigma}} v$ intersects $\Sigma_s^+$. Therefore, there is an open neighborhood $N \subset \widetilde{\Sigma}$ of $x$ such that $N \subset \mathrm{Vor}|_{\widetilde{\Sigma}} p$ and $N$ intersects no other cell. The same reasoning applies to points on $p_s^-$, $q_s^+$, and $q_s^-$. Hence $p_s^+$ and $p_s^-$ lie in the interior of $\mathrm{Vor}|_{\widetilde{\Sigma}} p$ and do not intersect another extended Voronoi cell. ◀

The shape of our extrusions $\Sigma_s^+$ and $\Sigma_s^-$ is motivated in part by Theorem 2, which justifies the word "constrained" in "restricted constrained Delaunay triangulation."

The following theorem shows that the sites whose extended Voronoi cells lie in part on an extrusion $\Sigma_s^+$ must lie in a ball (of modest radius) centered on the midpoint of the segment $s$. This helps us to efficiently compute the restricted CDT, because the portion of $\mathrm{Vor}|_{\widetilde{\Sigma}} V$ that lies on $\Sigma_s^+$ or $\Sigma_s^-$ depends only on sites near $s$.

▶ **Theorem 3** (Possession Theorem). *Let $s \in S$ be a segment with endpoints $p, q \in V$ such that $d(p,q) \le \rho\,\mathrm{lfs}(p)$ for $\rho \le 0.47$. Let $c$ be the midpoint of $s$. Let $v \in V$ be a site whose extended Voronoi cell $\mathrm{Vor}|_{\widetilde{\Sigma}} v$ contains a point $x \in \Sigma_s^+$ or $x \in \Sigma_s^-$. Then $v$ lies in the ball $B(c, \lambda\,\mathrm{lfs}(p))$ with center $c$ and radius $\lambda\,\mathrm{lfs}(p)$, where*

$$\lambda = \sqrt{1-2\rho}\left(1 - \sqrt{1 - \frac{\rho^2}{4\,(1-2\rho)}}\right) + \sqrt{(2-4\rho)\left(1 - \sqrt{1 - \frac{\rho^2}{4\,(1-2\rho)}}\right)}.$$

For the limiting case $\rho = 0.47$, $\lambda \doteq 0.4694$; $B(c, \lambda\,\mathrm{lfs}(p))$ has almost twice the radius of $s$.

## 4 Extended Voronoi cell boundaries

There are only two phenomena that can determine the boundary of an extended Voronoi cell. (1) Portions of a cell's boundary may be determined by hyperplanes, each hyperplane being equidistant from two sites. For example, a point on the boundaries of two cells $\mathrm{Vor}|_{\widetilde{\Sigma}} v$

and $\mathrm{Vor}|_{\widetilde{\Sigma}} w$ might lie on the hyperplane that orthogonally bisects the line segment $vw$. (2) Portions of a cell's boundary may be determined by a shadow cast by a portal. For example, consider a point $x \in \mathrm{Vor}|_{\widetilde{\Sigma}} v$ such that the line segment $xv$ intersects the boundary of a portal $P_s$. Portal boundaries do not block visibility; hence the set of points on $\widetilde{\Sigma}$ visible from $v$ is closed. But an infinitesimal perturbation of $x$ might cause $x$ to be no longer visible from $v$. If $x$ is in the principal branch, this may happen because the perturbed $xv$ intersects the relative interior of $P_s$; if $x$ is in a secondary branch, it may happen because the perturbed $xv$ no longer intersects $P_s$. We say that a portal *casts a shadow at* $x$ if $x \in \mathrm{Vor}|_{\widetilde{\Sigma}} v$ lies on the boundary of the points on $\widetilde{\Sigma}$ visible from $v$. A Voronoi cell $\mathrm{Vor}|_{\widetilde{\Sigma}} w$ is not necessarily closed, because its boundary might contain a shadow point $x \in \mathrm{Vor}|_{\widetilde{\Sigma}} v$ such that $\widehat{d}(v,x) < \widehat{d}(w,x)$.

The following theorem states sampling conditions under which the second phenomenon cannot happen, so the boundaries of all the extended Voronoi cells are determined solely by bisecting hyperplanes, all the extended Voronoi cells are closed point sets, and every point on $\widetilde{\Sigma}$ is in an extended Voronoi cell. For a site $v \in V$, $v$'s *principal Voronoi cell* $\mathrm{Vor}|_{\overline{\Sigma}_S} v = \overline{\Sigma}_S \cap \mathrm{Vor}|_{\widetilde{\Sigma}} v$ is the subset of $v$'s extended Voronoi cell in the principal branch, including the portal curves but excluding the remainder of the extrusions.

▶ **Theorem 4** (Shadow Theorem). *Let $S$ be a set of segments (with endpoints in $V$) such that for every segment $s = pq \in S$, $d(p,q) \le 0.47\,\mathrm{lfs}(p)$. Suppose that for every site $v \in V$ and every point $x$ in the principal Voronoi cell $\mathrm{Vor}|_{\overline{\Sigma}_S} v$, $d(v,x) \le \max\{\mathrm{lfs}(v), \mathrm{lfs}(x)\}$. (This last condition holds if $V$ is a constrained $\epsilon$-sample, as defined in Section 5, for some $\epsilon \le 1$.)*

*Then for every site $v \in V$ and every point $x$ in the extended Voronoi cell $\mathrm{Vor}|_{\widetilde{\Sigma}} v$, the relative interior of the line segment $xv$ does not intersect the boundary of a portal.*

▶ **Corollary 5.** *Under the conditions of Theorem 4, every extended Voronoi cell is a closed point set (closed with respect to the topological space $\widetilde{\Sigma}$ or $\widetilde{X}$).*

▶ **Corollary 6.** *Under the conditions of Theorem 4, for every site $v \in V$ and every point $x$ on the boundary of $\mathrm{Vor}|_{\widetilde{\Sigma}} v$, there is a site $w \in V \setminus \{v\}$ such that $x \in \mathrm{Vor}|_{\widetilde{\Sigma}} w$ and $d(v,x) = d(w,x)$.*

▶ **Corollary 7.** *Under the conditions of Theorem 4, if every connected component of $\Sigma$ contains at least one site in $V$, then every point on $\widetilde{\Sigma}$ is in at least one extended Voronoi cell.*

The proofs of the Shadow Theorem and its corollaries appear in the full-length article [17].

## 5 Topological guarantees

Here we introduce conditions under which a restricted CDT is homeomorphic to the surface $\Sigma$, with a view toward applications in guaranteed-quality surface mesh generation. The *nearest point map* $\nu$ (nu) maps a point $x \in \mathbb{R}^3 \setminus M$ to the point $\nu(x)$ nearest $x$ on $\Sigma$. We show that the nearest point map (with its domain restricted to $|\mathrm{Del}|_{\widetilde{\Sigma}} V|$) is a homeomorphism from the underlying space of the restricted CDT $\mathrm{Del}|_{\widetilde{\Sigma}} V$ to the surface $\Sigma$.

Our proof has three conditions: *a segment length condition*, that each segment $s \in S$ with endpoints $p$ and $q$ satisfies $d(p,q) \le 0.3647\,\mathrm{lfs}(p)$; a *sampling condition* requiring the sites $V$ to be sufficiently dense; and an *encroachment condition* that prevents vertices in $V$ from being too close to a segment, to prevent the possibility of triangles with excessively large circumcircles. We build on a long line of theoretical work for proving that certain triangulations are topologically correct approximations of surfaces [1, 2, 4, 5, 6, 8, 12, 14, 16], developed to support provably good algorithms for surface reconstruction and mesh generation. Many RDT-based surface mesh generation algorithms enforce a sampling condition by inserting new vertices on $\Sigma$ [6, 7, 11, 12, 22], and some support constraining segments by inserting additional

vertices that subdivide segments until the RDT naturally respects them [9, 10, 12, 15, 23]. Our three conditions can likewise be enforced by inserting new vertices, but restricted CDTs will often reduce the number of new vertices needed on the segments.

To understand the sampling condition, consider a surface $\Sigma \subset \mathbb{R}^3$ without boundary, a set of segments $S$ with their endpoints on $\Sigma$, and a set of portal curves $Z = \{\zeta_s : s \in S\}$. Recall the principal surface $\overline{\Sigma}_S$, defined in Section 2 to be the completion of $\Sigma - \bigcup_{s \in S} \operatorname{relint} \zeta_s$. We say that a finite vertex set $V \subset \Sigma$ is a *constrained $\epsilon$-sample of* $(\Sigma, S, Z)$ if $V$ contains every endpoint of every $s \in S$ and for every point $x \in \overline{\Sigma}_S$, there is a site $v \in V$ such that $\widehat{d}(x, v) \leq \epsilon \operatorname{lfs}(x)$. That is, the ball with center $x$ and radius $\epsilon \operatorname{lfs}(x)$ contains at least one site visible from $x$. Here, visibility and $\widehat{d}$ are as defined in Section 2.2; they are what differentiates a constrained $\epsilon$-sample from a standard $\epsilon$-sample. (If $S$ is empty, the two are the same.) Our homeomorphism proof requires that $V$ be a constrained 0.3202-sample of $(\Sigma, S, Z)$.

The encroachment condition applies only to restricted Delaunay triangles whose dual faces intersect an extrusion, as in Figure 6. (A triangle's dual face is usually a single point, called an extended Voronoi vertex, but our homeomorphism proof does not depend on it.) Let $\tau$ be such a triangle. The *circumradius* $r$ of $\tau$ is the radius of the unique circle that passes through $\tau$'s three vertices. Let $w$ be the vertex of $\tau$ at $\tau$'s largest plane angle. We require that $r \leq 0.3606 \operatorname{lfs}(w)$. The purpose of this restriction is to prevent the existence of "inverted" triangles in $\operatorname{Del}|_{\widetilde{\Sigma}} V$, which create *foldovers*, points where the nearest point map $\nu$ from $|\operatorname{Del}|_{\widetilde{\Sigma}} V|$ to $\Sigma$ is not locally injective (hence $\nu$ is not a homeomorphism).

To put the encroachment condition into perspective, suppose that $\Sigma$ is a sphere and consider a segment $s \in S$ having the maximum safe length of 0.3647 times the sphere's radius. A triangle $\tau$ whose dual vertex lies on $\Sigma_s^+$ can exceed the safe radius of 0.3606 times the sphere's radius only if $\tau$ has an angle greater than 149.62°. If $s$ is shorter, this angle is larger: in the limit as the segment lengths approach zero (or the radius of $\Sigma$ approaches infinity), the encroachment condition falls away and restricted CDTs on $\Sigma$ behave like CDTs in the plane. By contrast, in standard approaches using an RDT that conforms to the segments, no triangle with edge $s$ can have an angle opposite $s$ greater than 90°.

The sampling and encroachment conditions both rule out triangles with circumradii that are excessively large relative to the local feature size. A large circumradius implies either that the triangle is large, or that it has a large plane angle (close to 180°). Imposing these conditions is consistent with a mesh generator's goal of producing only well-shaped triangles, so our conditions are not onerous. Nevertheless, there are other applications such as surface reconstruction where the encroachment condition is not a natural condition. The restricted CDT may nevertheless still be useful in that context; see the Conclusions for speculations.

Our main topological result is the next theorem. Unfortunately, the proof is over twenty pages long; see the full-length article [17]. To keep the proof from being even longer, we assume that no point on $\widetilde{\Sigma}$ is equidistant from four visible vertices in $V$, which implies that no point is in more than three cells. (This assumption is not actually necessary.)

▶ **Theorem 8** (Homeomorphism). *Let $V$ be a constrained $\epsilon$-sample of $(\Sigma, S, Z)$ for some $\epsilon \leq 0.3202$. Suppose that for every segment $pq \in S$, $d(p, q) \leq 0.3647 \operatorname{lfs}(p)$. Suppose that no portal curve in $Z$ has a relative interior that intersects another portal curve in $Z$ or a site in $V$. Suppose that no point on $\widetilde{\Sigma}$ is equidistant from four visible vertices in $V$. Suppose that for every restricted Delaunay triangle $\tau$ whose dual extended Voronoi face intersects an extrusion, $\tau$ satisfies $r \leq 0.3606 \operatorname{lfs}(w)$, where $r$ is $\tau$'s circumradius and $w$ is the vertex of $\tau$ at $\tau$'s largest plane angle. Then the nearest point map $\nu : |\operatorname{Del}|_{\widetilde{\Sigma}} V| \to \Sigma$ is a homeomorphism.*

The proof is related to proofs by Amenta et al. [3] and Boissonnat and Ghosh [5] that also use the nearest point map. We sketch a few ideas. To make every extended Voronoi cell become a topological disk and to clarify the duality between the extended Voronoi diagram and the restricted CDT, it is convenient to define a compact 2-manifold without boundary $\mathring{\widetilde{\Sigma}}$, obtained from $\widetilde{\Sigma}$ by gluing each pair $\Sigma_s^+$ and $\Sigma_s^-$ together along their boundaries as illustrated in Figure 7. For each segment $s = pq$, we topologically identify the ray $p_s^+$ with the ray $p_s^-$, and $q_s^+$ with $q_s^-$. (Theorem 2 shows that $p_s^+$ and $p_s^-$ are subsets of $p$'s extended Voronoi cell, so this gluing does not confuse which points are in which Voronoi cell.) We create a single point $s^\infty$ "at infinity" (one such point per segment $s$) at the end of every ray $x_s^+$ and $x_s^-$ for all $x \in \zeta_s$, thereby making $\mathring{\widetilde{\Sigma}}$ compact. Thus the hole created in $\overline{\Sigma}_S$ by cutting a slit at $\zeta_s$ is filled in $\mathring{\widetilde{\Sigma}}$ with a topological disk $\Sigma_s^+ \cup \Sigma_s^- \cup s^\infty$, as illustrated. Clearly, $\mathring{\widetilde{\Sigma}}$ is homeomorphic to $\Sigma$. (Note that unlike $\widetilde{\Sigma}$, $\mathring{\widetilde{\Sigma}}$ is not embedded in $\widetilde{X}$ and has neither coordinates nor distances.)

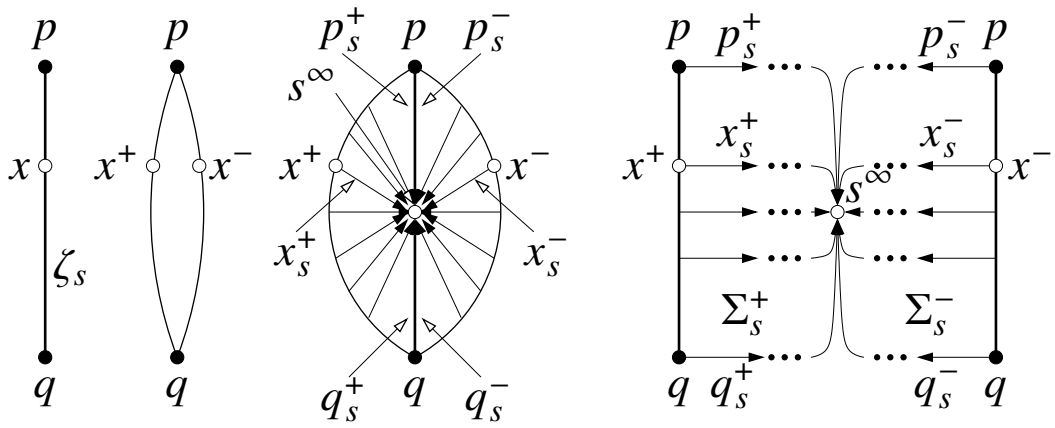


**Figure 7** After we remove relint $\zeta_s$ from $\Sigma$, we glue two extrusions $\Sigma_s^+$ and $\Sigma_s^-$ in the hole to create $\widetilde{\Sigma}$. Additional gluing can transform $\widetilde{\Sigma}$ into a compact 2-manifold without boundary $\mathring{\widetilde{\Sigma}}$, restoring the topology of $\Sigma$, by gluing the ray $p_s^+$ to $p_s^-$, gluing $q_s^+$ to $q_s^-$, and filling the hole with a point $s^\infty$.

If $V$ is a constrained 0.44-sample and $S$ satisfies the segment length condition, we show that every extended Voronoi cell on $\mathring{\widetilde{\Sigma}}$ is homeomorphic to a closed disk. With the assumption that no point is in more than three cells, this implies that the adjacency graph of $\mathrm{Vor}|_{\widetilde{\Sigma}} V$, which is the graph of $\mathrm{Del}|_{\widetilde{\Sigma}} V$, can be drawn on $\mathring{\widetilde{\Sigma}}$ (and therefore on $\widetilde{\Sigma}$) with no crossings.

We call an extended Voronoi vertex a *principal vertex* if it lies in the principal branch (on $\overline{\Sigma}_S$), or a *secondary vertex* if it lies on an extrusion but not on a portal curve. We show that if $V$ is a constrained 0.3202-sample, each principal vertex dualizes to a triangle whose circumradius is not large (relative to the local feature size). The encroachment condition implies that each secondary vertex dualizes to a triangle whose circumradius is not large.

The bounds on circumradii allow us to prove that the nearest point map restricted to any single restricted Delaunay triangle is a homeomorphism. Moreover, there is a sense in which the map preserves orientation: for any extended Voronoi vertex $u$ whose dual extended Delaunay triangle is $\tau = \triangle pp'p''$, the sites $p$, $p'$, and $p''$ are in counterclockwise order around $v(\tau)$ if and only if the cells $\mathrm{Vor}|_{\widetilde{\Sigma}} p$, $\mathrm{Vor}|_{\widetilde{\Sigma}} p'$, and $\mathrm{Vor}|_{\widetilde{\Sigma}} p''$ adjoin $u$ in counterclockwise order around $u$ (as seen from outside $\Sigma$). From this, we argue that along each of its edges, each restricted Delaunay triangle adjoins another restricted Delaunay triangle with a consistent orientation, and therefore the triangles must cover the whole surface $\Sigma$ – that is, the nearest point map is a surjection from $|\mathrm{Del}|_{\widetilde{\Sigma}} V|$ to $\Sigma$. As the boundary of a Voronoi cell $\mathrm{Vor}|_{\widetilde{\Sigma}} v$ is a simple loop, the restricted Delaunay triangles adjoining $v$ form a fan of triangles around $v$ whose union is a topological disk. From these facts we prove that the nearest point map is an injection from $|\mathrm{Del}|_{\widetilde{\Sigma}} V|$ to $\Sigma$ (there are no foldovers) and therefore a homeomorphism.

## 6 Conclusions

The restricted constrained Delaunay triangulation is a rigorous generalization of the constrained Delaunay triangulation to surfaces. Under suitable conditions on the vertex density and the segment lengths, the restricted CDT is homeomorphic to $\Sigma$ and contains every constraining segment. We believe that the restricted CDT will become a useful tool for enforcing specified boundaries in guaranteed-quality algorithms for surface meshing. But first and foremost, we think the existence of restricted CDTs is a beautiful mathematical fact.

Several algorithms suggest themselves for computing the restricted CDT. The classical gift-wrapping algorithm [12, Section 3.11] [25] can be adapted. Another approach, likely faster in practice, is to start with the RDT and then incrementally insert the segments one by one [27]. It is an open problem to design an algorithm that runs in $O(|V|^2)$ time or better.

Another open problem is to design a guaranteed-quality algorithm that uses the restricted CDT to mesh surfaces with prescribed boundaries. The algorithm must generate new vertices on $\Sigma$ with the goal of enforcing the sampling and encroachment conditions, in addition to the customary goal of constructing high-quality triangles. As we have said, we believe that restricted CDTs will require fewer triangles and vertices than algorithms based on RDTs.

Although our encroachment condition is reasonable in a surface mesh generator, it is undesirable in some applications such as surface reconstruction. Unfortunately, without this condition, we cannot prove a homeomorphism because the nearest point map is not necessarily injective. Figure 8 illustrates the problem. Suppose that we place two segments $s$ and $s'$ close together and we place a vertex $r$ very close to the midpoint of $\zeta_{s'}$ (violating the encroachment condition), as shown in Figure 8. Consider the triangle formed by $r$ and $s'$, and its dual 3D Voronoi edge $e$; $e$ can be arbitrarily close to perpendicular to $P_{s'}$. Then $e$ may enter both portals $P_s$ and $P_{s'}$ and generate two extended Voronoi vertices (illustrated in red) where it intersects $\Sigma^+_{s'}$ (which is desirable) and $\Sigma^+_s$ (which is not). This circumstance is possible because the segments are close together, the portals are tilted toward each other, and $\Sigma^+_s$ is extruded infinitely far. Increasing the sampling density does not fix this problem.

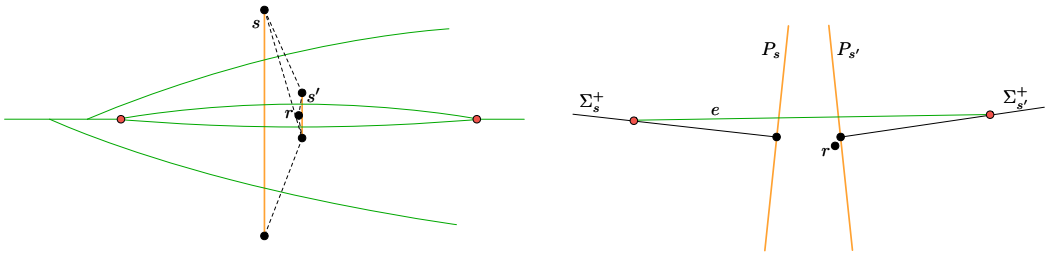


**Figure 8** The left figure shows a top view of a Voronoi diagram drawn on $\widetilde{\Sigma}$; the right figure shows a side view. The segments $s$ and $s'$ are placed close together on $\Sigma$ and their portals $P_s$ and $P_{s'}$ are tilted toward each other in the side view. If $r$ is arbitrarily close to $P_{s'}$, the Voronoi edge $e$ dual to $\triangle rs'$ is tilted nearly tangent to the surface and can leave $P_{s'}$, enter $P_s$, and intersect $\Sigma^+_s$ (perhaps far down the extrusion). The dual triangulation contains a dangling triangle $\triangle rs'$.

If we drop the encroachment condition (but retain the other two conditions), we conjecture that the restricted Delaunay triangles still form a watertight enclosure such that the nearest point map is a surjection from the restricted CDT to $\Sigma$. However, it is not necessarily injective; there may be foldovers where sites brush up against segments. There may also be "dangling" triangles, connected to the remainder of the triangulation by only a single edge; an example is the triangle formed by $r$ and $s'$ in Figure 8. Such triangles are easily pruned.

## References


1 Nina Amenta and Marshall Bern. Surface Reconstruction by Voronoi Filtering. *Discrete & Computational Geometry*, 22(4):481–504, June 1999.

2 Nina Amenta, Marshall W. Bern, and David Eppstein. The Crust and the $\beta$-Skeleton: Combinatorial Curve Reconstruction. *Graphical Models and Image Processing*, 60(2):125–135, March 1998.

3 Nina Amenta, Sunghee Choi, Tamal K. Dey, and Naveen Leekha. A Simple Algorithm for Homeomorphic Surface Reconstruction. *International Journal of Computational Geometry and Applications*, 12(1–2):125–141, 2002.

4 Jean-Daniel Boissonnat, Frédéric Chazal, and Mariette Yvinec. *Geometric and Topological Inference*, volume 57. Cambridge University Press, September 2018.

5 Jean-Daniel Boissonnat and Arijit Ghosh. Manifold Reconstruction Using Tangential Delaunay Complexes. *Discrete & Computational Geometry*, 51(1):221–267, 2014.

6 Jean-Daniel Boissonnat and Steve Oudot. Provably Good Surface Sampling and Approximation. In *Symposium on Geometry Processing*, pages 9–18. Eurographics Association, June 2003.

7 Jean-Daniel Boissonnat and Steve Oudot. Provably Good Sampling and Meshing of Surfaces. *Graphical Models*, 67(5):405–451, September 2005.

8 Ho-Lun Cheng, Tamal K. Dey, Herbert Edelsbrunner, and John Sullivan. Dynamic Skin Triangulation. *Discrete & Computational Geometry*, 25(4):525–568, December 2001.

9 Siu-Wing Cheng, Tamal K. Dey, and Joshua A. Levine. A Practical Delaunay Meshing Algorithm for a Large Class of Domains. In *Proceedings of the 16th International Meshing Roundtable*, pages 477–494, Seattle, Washington, October 2007.

10 Siu-Wing Cheng, Tamal K. Dey, and Edgar A. Ramos. Delaunay Refinement for Piecewise Smooth Complexes. *Discrete & Computational Geometry*, 43(1):121–166, 2010.

11 Siu-Wing Cheng, Tamal K. Dey, Edgar A. Ramos, and Tathagata Ray. Sampling and Meshing a Surface with Guaranteed Topology and Geometry. *SIAM Journal on Computing*, 37(4):1199–1227, 2007.

12 Siu-Wing Cheng, Tamal Krishna Dey, and Jonathan Richard Shewchuk. *Delaunay Mesh Generation*. CRC Press, Boca Raton, Florida, 2012.

13 L. Paul Chew. Constrained Delaunay Triangulations. *Algorithmica*, 4(1):97–108, 1989.

14 Tamal K. Dey. *Curve and Surface Reconstruction: Algorithms with Mathematical Analysis*. Cambridge University Press, New York, 2007.

15 Tamal K. Dey and Joshua A. Levine. Delaunay Meshing of Piecewise Smooth Complexes without Expensive Predicates. *Algorithms*, 2(4):1327–1349, 2009.

16 Herbert Edelsbrunner and Nimish R. Shah. Triangulating Topological Spaces. *International Journal of Computational Geometry and Applications*, 7(4):365–378, 1997.

17 Marc Khoury and Jonathan Richard Shewchuk. Restricted Constrained Delaunay Triangulations. The complete version of this paper, March 2021. URL: `https://people.eecs.berkeley.edu/~jrs/papers/rcdt.pdf`.

18 Ron Kimmel and James A. Sethian. Computing Geodesic Paths on Manifolds. *Proceedings of the National Academy of Sciences*, 95(15):8431–8435, July 1998.

19 Der-Tsai Lee and Arthur K. Lin. Generalized Delaunay Triangulations for Planar Graphs. *Discrete & Computational Geometry*, 1:201–217, 1986.

20 Takashi Maekawa. Computation of Shortest Paths on Free-Form Parametric Surfaces. *Journal of Mechanical Design*, 118(4):499–508, December 1996.

21 Manish Mandad, David Cohen-Steiner, Leif Kobbelt, Pierre Alliez, and Mathieu Desbrun. Variance-Minimizing Transport Plans for Inter-Surface Mapping. *ACM Transactions on Graphics*, 36(4), 2017.

22 Steve Oudot, Laurent Rineau, and Mariette Yvinec. Meshing Volumes Bounded by Smooth Surfaces. In *Proceedings of the 14th International Meshing Roundtable*, pages 203–219, San Diego, California, September 2005. Springer.

23 Laurent Rineau and Mariette Yvinec. Meshing 3D Domains Bounded by Piecewise Smooth Surfaces. In *Proceedings of the 16th International Meshing Roundtable*, pages 443–460, Seattle, Washington, 2007. Springer.

24 Erich Schönhardt. Über die Zerlegung von Dreieckspolyedern in Tetraeder. *Mathematische Annalen*, 98:309–312, 1928.

25 Raimund Seidel. Constrained Delaunay Triangulations and Voronoi Diagrams with Obstacles. In H. S. Poingratz and W. Schinnerl, editors, *1978–1988 Ten Years IIG*, pages 178–191. Institute for Information Processing, Graz University of Technology, 1988.

26 Jonathan Richard Shewchuk. Delaunay Refinement Algorithms for Triangular Mesh Generation. *Computational Geometry: Theory and Applications*, 22(1–3):21–74, 2002.

27 Jonathan Richard Shewchuk and Brielin C. Brown. Fast Segment Insertion and Incremental Construction of Constrained Delaunay Triangulations. *Computational Geometry: Theory and Applications*, 48(8):554–574, 2015.